PROCEEDINGS OF SCIENCE

Higgs boson production and properties at ATLAS: decays into boson pairs, and overall combination

Zef Wolffs,[a,b] **on behalf of the ATLAS Collaboration**

[a] *Insitute of Physics, University of Amsterdam, Amsterdam, the Netherlands*

[a] *ATLAS Group, Nikhef, Amsterdam, the Netherlands*

E-mail: zef.wolffs@nikhef.nl

Combining individual measurements of Higgs boson properties provides enhanced sensitivity and enables precise tests of the Standard Model. These proceedings present a recent combination of ATLAS analyses based on the full LHC Run 2 dataset comprising 140 fb^{-1} at 13 TeV, yielding the most precise ATLAS results so far of Higgs boson couplings and production and decay cross-sections. In addition, four dedicated analyses of Higgs boson decays to (vector) bosons are discussed. Two of these focus on $H \to WW^*$ using the full Run 2 dataset, while the other two present the first Run 3 measurements of $H \to ZZ^*$ with 56 fb^{-1} of early data collected at $\sqrt{s}$ = 13.6 TeV. All results presented agree with predictions, attesting to the remarkable precision with which the Higgs boson continues to conform to the Standard Model expectations.

The European Physical Society Conference on High Energy Physics (EPS-HEP2025)
7-11 July 2025
Marseille, France

 ISSN 1824-8039 . Published by SISSA Medialab.

PoS(EPS-HEP2025)060

1. Introduction

Since the discovery of the Higgs boson in 2012 [2, 3], understanding its properties has remained one of the central goals of the LHC physics programme. While the Standard Model (SM) makes precise predictions for Higgs boson couplings, production and decay rates, many of these have not yet been measured with sufficient precision to rule out possible deviations. Any departure from SM expectations could provide the first indication of new physics.

A particularly powerful strategy for probing Higgs boson properties is to combine multiple individual measurements into a single global analysis. Individual analyses typically focus on a specific production or decay mode and use only a subset of the full dataset, while a combination exploits the statistical power of the entire dataset and provides a coherent treatment of correlated systematic uncertainties. The ATLAS [1] Run 2 Higgs boson combination presented in these proceedings uses the full 140 fb^{-1} of pp collision data at $\sqrt{s}$ = 13 TeV, delivering the most precise measurements of Higgs boson couplings and cross-sections to date [6].

In addition to the combination, this work discusses four dedicated analyses of Higgs boson decays to vector bosons and photons in fully leptonic final states. Two of these target the $H \to WW^*$ decay mode, one focusing on gluon gluon fusion (ggF) and vector boson fusion (VBF) production [8], and the other on associated production with a vector boson (VH) [9]. Both are based on the complete Run 2 dataset and provide sensitivity to Higgs boson production mechanisms. The other two analyses focus on $H \to ZZ^* \to 4\ell$, using the first Run 3 data collected in 2022–2023 [21, 22]. While the $H \to WW^*$ decay has a higher branching fraction, the presence of neutrinos in the final state limits the achievable precision. In contrast, the $H \to ZZ^* \to 4\ell$ channel offers a fully reconstructible final state with excellent mass resolution, making it the *golden channel* for precision measurements, and therefore the natural choice for the first Run 3 studies. These results mark the beginning of Higgs boson measurements at the increased LHC centre-of-mass energy of 13.6 TeV, compared to 13 TeV in Run 2.

2. Higgs combination

Both the ATLAS and CMS collaborations published comprehensive combinations of Higgs boson measurements in 2022, marking ten years since its discovery [4, 5]. Since then, several new ATLAS analyses have been completed, providing additional sensitivity and warranting an updated combination. That updated combination, based on the full Run 2 dataset, is presented here [6].

The combination includes all major Higgs boson production mechanisms: gluon gluon fusion (ggF), vector-boson fusion (VBF), associated production with a vector boson (VH), and associated production with heavy quarks ($t\bar{t}H$, bbH, and tH). The decay channels considered are $H \to b\bar{b}$, $H \to WW^* \to \ell\nu\ell\nu$, $H \to \tau\tau$, $H \to c\bar{c}$, $H \to ZZ^* \to 4\ell$, $H \to \gamma\gamma$, $H \to Z\gamma$, and $H \to \mu\mu$. Compared to the 2022 ATLAS combination [4], six channels are either new or updated, leading to substantial improvements in the precision of the $H \to \tau\tau$, $H \to WW^*$, $VH(\to b\bar{b}, c\bar{c})$, and $t\bar{t}H(\to b\bar{b})$ results. A full overview of the inputs to the combination is given in Table 1.

The results are interpreted in several ways. A global measurement of the signal strength parameter,

$$\mu = 1.023^{+0.056}_{-0.053} = 1.023 \pm 0.028\ (\text{stat.})^{+0.026}_{-0.025}\ (\text{exp.})^{+0.039}_{-0.036}\ (\text{sig. theo.}) \pm 0.012\ (\text{bkg. theo.}),$$

Table 1: Summary of the analyses entering the combination, listing their integrated luminosity ($\mathcal{L}$), bibliographic reference, and type of improvement relative to the combination in Ref. [4]. Results originally quoted at 139 fb^{-1} have been uniformly rescaled to the updated Run 2 value of 140 fb^{-1}. The last column specifies whether an input is a *New analysis*, an updated *Full Run 2* result, or a *Reanalysis* [6].

Analysis	Prod.	$\mathcal{L}$ (fb^{-1})	Reference	Improvements
$H \to ZZ^* \to 4\ell$	All	140	[7]	-
$H \to WW^* \to \ell\nu\ell\nu$	ggF,VBF	140	[8]	Reanalysis
$H \to WW^* \to \ell\nu\ell\nu$	VH	140	[9]	Full Run 2
$H \to \gamma\gamma$	All	140	[10]	-
$H \to Z\gamma$	All	140	[11]	-
$H \to \tau\tau$	All	140	[12]	Reanalysis
$H \to \tau\tau$	VH	140	[13]	New analysis
$H \to \mu\mu$	All	140	[14]	-
$H \to bb$	VBF	126	[15]	-
$H \to bb, cc$	VH	140	[16]	Reanalysis
$H \to$ multileptons	ttH	36.1	[17]	-
$H \to bb$	ttH	140	[18]	Reanalysis

quantifies the overall Higgs boson production and decay rate relative to the (SM). The result is in agreement with the SM expectation of $1.000^{+0.055}_{-0.053}$.

Beyond this single parameter, 29 combinations of production cross-sections σ_i and branching ratios B_f are extracted simultaneously, providing a detailed mapping of Higgs boson interactions across production and decay channels, and showing good agreement with SM predictions with a p-value of $p_{SM} = 84\%$. A κ-framework interpretation [19] is also performed, in which modifiers κ_i are applied to the Higgs boson couplings to SM particles. The updated dataset brings notable improvements compared to the 2022 combination, with the precision on κ_c improving by roughly a factor of two, and κ_t improving by about 15%. The full set of coupling modifiers is shown in Figure 1.

Overall, all measurements are consistent with SM expectations, and the increased precision highlights the remarkable agreement of Higgs boson properties with the SM more than a decade after its discovery.

3. Measurements of $H \to WW$ in Run 2

Two of the new inputs to the combination described in the previous section are dedicated analyses in the $H \to WW^*$ decay channel using the full LHC Run 2 dataset, and are further discussed here.

The first analysis focuses on VH production with subsequent $H \to WW^*$ decays [9]. Events with two, three, or four charged leptons are considered, corresponding to the leptonic decays of the associated vector boson and the W bosons from the Higgs boson decay. A multivariate approach is employed in each channel, combining neural networks and boosted decision trees to discriminate

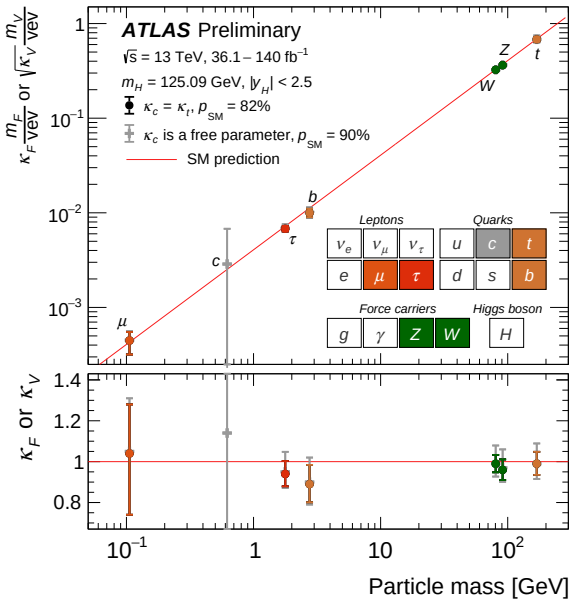

Figure 1: Summary of Higgs boson coupling modifiers to fermions and bosons as a function of particle mass. The upper panel displays $\kappa_F m_F/v$ for fermions and $\sqrt{\kappa_V} m_V/v$ for vector bosons, with $v = 246$ GeV the Higgs vacuum expectation value. Fermion masses are taken in the $\overline{\text{MS}}$ scheme at m_H, while pole masses are used elsewhere. The lower panel shows the extracted values of the coupling modifiers κ. Results are provided for two scenarios: one with κ_c treated as an independent parameter (light markers) and one where κ_c is assumed equal to κ_t (dark markers) [6].

the Higgs boson signal from backgrounds. The sum of the WH and ZH cross sections times the $H \to WW^*$ branching ratio is measured to be

$$\sigma_{VH} \times B(H \to WW^*) = 0.44^{+0.10}_{-0.09}\ (\text{stat.})^{+0.06}_{-0.05}\ (\text{syst.})\ \text{pb},$$

in agreement with the SM prediction of $\sigma^{\text{SM}}_{VH} \times B(H \to WW^*) = 0.48 \pm 0.01$ pb. Differential cross sections are also extracted in the Simplified Template Cross Section (STXS) framework [20] and in a dedicated measurement of the vector boson transverse momentum, p^V_{T}. While the STXS scheme already includes p^V_{T}-defined bins, the dedicated p^V_{T} measurement is otherwise inclusive and employs a finer binning, providing complementary sensitivity. The limiting factor in these measurements is the statistical uncertainty. Thus, the increase in the number of events collected in Run 3 is expected to significantly improve the sensitivity of this analysis.

The second analysis targets ggF and VBF production in the $H \to WW^* \to \ell\nu\ell\nu$ channel [8]. Events are categorised according to jet multiplicity, with dedicated deep neural network discriminants trained to optimise signal separation in each topology. The measured inclusive cross-sections times branching ratio are

$$\sigma_{\text{ggF}} \times B(H \to WW^*) = 12.4^{+1.3}_{-1.2}\ \text{pb} \quad \text{and} \quad \sigma_{\text{VBF}} \times B(H \to WW^*) = 0.79^{+0.18}_{-0.16}\ \text{pb},$$

which are both in good agreement with the SM predictions of 10.4 ± 0.6 pb and 0.81 ± 0.02 pb, respectively. For the ggF measurement, no single source of uncertainty is dominant: statistical

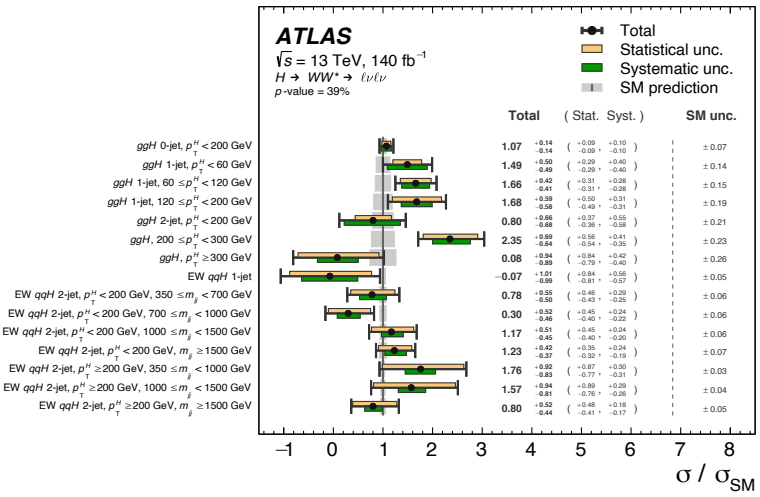

Figure 2: Measured $H \to WW^*$ cross-sections in the STXS categories, normalised to the SM predictions. Error bars show the total uncertainties, with the upper bands indicating the statistical components, and the lower bands the systematic components. The shaded areas represent the theoretical uncertainty on the predicted yields [8].

and systematic components are of similar size, with systematic experimental effects such as muon reconstruction and flavour tagging (important for suppressing b-jet backgrounds) providing notable contributions. In contrast, the VBF measurement is primarily limited by statistical uncertainties and uncertainties in the theoretical modelling of the VBF signal.

In addition to the inclusive two-parameter fit, differential measurements are performed in 15 STXS fiducial regions, as shown in Figure 2. These results are also interpreted in the framework of the Standard Model Effective Field Theory (SMEFT), using a modified STXS categorisation designed to gain sensitivity to CP-odd effects. Constraints are obtained on both CP-even and CP-odd dimension-six operators modifying the Higgs boson interactions, with all observed results remaining consistent with SM expectations.

Together, these analyses consolidate the ATLAS Run 2 programme in the $H \to WW^*$ decay channel, achieving precise cross-section measurements across multiple production modes and providing direct tests of the structure of Higgs boson interactions.

4. Early Run 3 measurements of $H \to ZZ$ and $H \to \gamma\gamma$

The first ATLAS Higgs boson measurements at a centre-of-mass energy of $\sqrt{s} = 13.6$ TeV were performed using the $H \to ZZ^* \to 4\ell$ and $H \to \gamma\gamma$ channels [21]. The dataset used in the measurement of the $H \to \gamma\gamma$ channel was recorded in 2022, corresponding to an integrated luminosity of 31.4 fb^{-1}. This analysis measures an inclusive fiducial cross-section of $\sigma_{\text{fid}}(H \to \gamma\gamma) = 76^{+14}_{-13}$ fb, in agreement with the SM prediction of 67.6 ± 3.7 fb. The fiducial region is defined by the requirement on the rapidity of the Higgs boson, y_H, to be below 2.5. After extrapolation to the full phase space, the corresponding total Higgs boson production cross-section is $\sigma(pp \to H) = 58.2 \pm 8.7$ pb, consistent with the SM expectation of 59.9 ± 2.6 pb.

A subsequent ATLAS analysis of 56 fb^{-1} of Run 3 data, including data collected in 2023, measures the $H \to ZZ^* \to 4\ell$ final state [22]. The inclusive fiducial cross-section is measured as $\sigma_{\text{fid}} = 3.5^{+0.6}_{-0.5}$ fb, consistent with the SM prediction of 3.7 ± 0.1 fb, corresponding to a total cross-section of $\sigma_{\text{tot}} = 57^{+10}_{-9}$ pb. The fiducial region is defined at particle level to mirror the reconstruction-level selection, using electrons and muons within $|\eta| < 2.7$ and p_{T} thresholds of 7 and 5 GeV, respectively, and requiring a Higgs boson candidate formed from two same-flavour opposite-charge lepton pairs. In addition, differential cross-sections are presented in bins of the Higgs boson transverse momentum, rapidity, the invariant mass of the off-shell lepton pair, and jet multiplicity. For the first time at $\sqrt{s} = 13.6$ TeV, cross-sections for individual production modes (ggF, VBF, VH, $t\bar{t}H$) are extracted, and interpretations are performed both in terms of constaints on Higgs coupling strength modifiers and coefficients for SMEFT CP-even and CP-odd operators. All results are compatible with SM predictions.

In both the $H \to ZZ^* \to 4\ell$ and $H \to \gamma\gamma$ channels, the measurements are primarily limited by statistical uncertainties, reflecting the modest size of the early Run 3 dataset.

Together, these early Run 3 measurements provide a first validation of the SM predictions at a collision energy of 13.6 TeV, and open the path towards precision Higgs boson studies with the much larger dataset expected in the coming years.

5. Conclusion

The Higgs boson continues to be scrutinised with ever-increasing precision at the LHC. The ATLAS Run 2 Higgs boson combination presented here provides the most comprehensive ATLAS measurement to date of production and decay cross-sections, as well as constraints on Higgs boson couplings within the κ-framework. Two recently published dedicated analyses of $H \to WW^*$ are used in this combination, and contribute with precise cross-section determinations across multiple production mechanisms.

Early Run 3 analyses in $H \to ZZ^* \to 4\ell$ and $H \to \gamma\gamma$ mark the beginning of Higgs boson measurements at $\sqrt{s} = 13.6$ TeV, confirming the consistency of Higgs boson production and decay with SM expectations at this new center-of-mass energy, and for the first time combining Run 2 and Run 3 data in a coupling interpretation.

Altogether, these results underline the remarkable agreement of Higgs boson properties with SM predictions, while setting the stage for the much larger Run 3 dataset to probe Higgs boson interactions with unprecedented sensitivity. The continued improvement of experimental techniques and theoretical precision will be crucial in searching for possible deviations that may reveal new physics beyond the Standard Model.

References

[1] ATLAS Collaboration, *The ATLAS Experiment at the CERN Large Hadron Collider*, JINST **3**, S08003 (2008), arXiv:2305.16623 [physics.ins-det].

[2] ATLAS Collaboration, *Observation of a new particle in the search for the Standard Model Higgs boson with the ATLAS detector at the LHC*, Phys. Lett. B **716**, 1–29 (2012), arXiv:1207.7214 [hep-ex].

[3] CMS Collaboration, *Observation of a new boson at a mass of 125 GeV with the CMS experiment at the LHC*, Phys. Lett. B **716**, 30–61 (2012), arXiv:1207.7235 [hep-ex].

[4] ATLAS Collaboration, *A detailed map of Higgs boson interactions by the ATLAS experiment ten years after the discovery*, Nature **607**, 52–59 (2022).

[5] CMS Collaboration, *A portrait of the Higgs boson by the CMS experiment ten years after the discovery*, Nature **607**, 60–68 (2022).

[6] ATLAS Collaboration, *Combined measurements of Higgs boson production and decay at* $\sqrt{s} = 13$ *TeV using up to 140* fb^{-1} *of data collected by the ATLAS experiment*, ATLAS-CONF-2025-006, https://cds.cern.ch/record/2937634 (2025).

[7] ATLAS Collaboration, *Higgs boson production cross-section measurements and their EFT interpretation in the* 4ℓ *decay channel at* $\sqrt{s} = 13$ *TeV with the ATLAS detector*, Eur. Phys. J. C **80**, 957 (2020), arXiv:2004.03447 [hep-ex]; Erratum: Eur. Phys. J. C **81**, 29 (2021); Erratum: Eur. Phys. J. C **81**, 398 (2021).

[8] ATLAS Collaboration, *Measurements of Higgs boson production via gluon gluon fusion and vector-boson fusion using* $H \to WW^* \to \ell\nu\ell\nu$ *decays in pp collisions with the ATLAS detector and their effective field theory interpretations*, submitted to Eur. Phys. J. C, arXiv:2504.07686 [hep-ex] (2025).

[9] ATLAS Collaboration, *Measurements of the production cross-sections of a Higgs boson in association with a vector boson and decaying into* WW^* *with the ATLAS detector at* $\sqrt{s} = 13$ *TeV*, JHEP 08 (2025) 034, arXiv:2503.19420 [hep-ex].

[10] ATLAS Collaboration, *Measurement of the properties of Higgs boson production at* $\sqrt{s} = 13$ *TeV in the* $H \to \gamma\gamma$ *channel using* 139 fb^{-1} *of pp collision data with the ATLAS experiment*, JHEP **07** (2023) 088, arXiv:2207.00348 [hep-ex].

[11] ATLAS Collaboration, *A search for the* $Z\gamma$ *decay mode of the Higgs boson in pp collisions at* $\sqrt{s} = 13$ *TeV with the ATLAS detector*, Phys. Lett. B **809**, 135754 (2020), arXiv:2005.05382 [hep-ex].

[12] ATLAS Collaboration, *Differential cross-section measurements of Higgs boson production in the* $H \to \tau^+\tau^-$ *decay channel in pp collisions at* $\sqrt{s} = 13$ *TeV with the ATLAS detector*, JHEP **03** (2025) 010, arXiv:2407.16320 [hep-ex].

[13] ATLAS Collaboration, *Measurement of the* VH, $H \to \tau\tau$ *process with the ATLAS detector at 13 TeV*, Phys. Lett. B **855**, 138817 (2024), arXiv:2312.02394 [hep-ex].

[14] ATLAS Collaboration, *A search for the dimuon decay of the Standard Model Higgs boson with the ATLAS detector*, Phys. Lett. B **812**, 135980 (2021), arXiv:2007.07830 [hep-ex].

[15] ATLAS Collaboration, *Measurements of Higgs bosons decaying to bottom quarks from vector boson fusion production with the ATLAS experiment at* $\sqrt{s} = 13$ *TeV*, Eur. Phys. J. C **81**, 537 (2021), arXiv:2011.08280 [hep-ex].

[16] ATLAS Collaboration, *Measurements of WH and ZH production with Higgs boson decays into bottom quarks and direct constraints on the charm Yukawa coupling in 13 TeV pp collisions with the ATLAS detector*, JHEP **04**, 075 (2025), arXiv:2410.19611 [hep-ex].

[17] ATLAS Collaboration, *Evidence for the associated production of the Higgs boson and a top quark pair with the ATLAS detector*, Phys. Rev. D **97**, 072003 (2018), arXiv:1712.08891 [hep-ex].

[18] ATLAS Collaboration, *Measurement of the associated production of a top-antitop-quark pair and a Higgs boson decaying into a $b\bar{b}$ pair in pp collisions at $\sqrt{s}$ = 13 TeV using the ATLAS detector at the LHC*, Eur. Phys. J. C **85**, 210 (2025), arXiv:2407.10904 [hep-ex].

[19] LHC Higgs Cross Section Working Group, *Handbook of LHC Higgs Cross Sections: 3. Higgs Properties*, CERN-2013-004 (2013).

[20] N. Berger et al., *Simplified Template Cross Sections – Stage 1.1*, arXiv:1906.02754 [hep-ph] (2019).

[21] ATLAS Collaboration, *Measurement of the $H \to \gamma\gamma$ and $H \to ZZ^* \to 4\ell$ cross-sections in pp collisions at $\sqrt{s}$ = 13.6 TeV with the ATLAS detector*, Eur. Phys. J. C **84**, 78 (2024), arXiv:2306.11379 [hep-ex].

[22] ATLAS Collaboration, *Measurements and interpretation of the Higgs boson differential and production mode cross sections in the $H \to ZZ^* \to 4\ell$ channel at $\sqrt{s}$ = 13.6 TeV with the ATLAS detector*, ATLAS-CONF-2025-002 (2025).